Electronics and Electrical Engineering

AIMS Electronics and Electrical Engineering, 10(2): 368–394.
DOI: 10.3934/electreng.2026015
Received: 01 November 2025
Revised: 19 March 2026
Accepted: 30 March 2026
Published: 12 May 2026

https://www.aimspress.com/journal/ElectrEng

Research article

Tracking control of wind-photovoltaic-storage hybrid system under uncertainty in renewable power generation

Yujing Shi[1], Mifeng Ren[1], Lan Cheng[1], Jianhua Zhang[2] and Junghui Chen[3,*]

[1] College of Electrical and Power Engineering, Taiyuan University of Technology, Taiyuan 030024, China
[2] State Key Laboratory of Alternate Electrical Power System with Renewable Energy Sources, North China Electric Power University, Beijing, China
[3] Department of Chemical Engineering, Chung-Yuan Christian University, Chung-Li, Taoyuan, Taiwan 32032, Republic of China

* **Correspondence:** Email: jason@wavenet.cycu.edu.tw; Tel: +886 3-265-4107.

Abstract: Accurately tracking planned output is a core requirement for ensuring the stable grid connection of hybrid wind-photovoltaic-storage systems. However, the strong randomness of wind and solar power output not only affects the tracking accuracy but also leads to frequent charge and discharge cycles of the energy storage system, thereby shortening its service life. To address this, we propose a control method for the energy storage system that accounts for wind and solar uncertainty, with the dual objectives of improving the planned output tracking performance and extending the energy storage system lifespan. By optimally controlling the charge and discharge of the energy storage system, this method enables the output of the hybrid wind-photovoltaic-storage system to track the planned output. The approach models wind and solar power joint distribution using Copula functions and applies K-means clustering to extract representative scenarios, reducing computational complexity. An interval control mechanism defines acceptable deviation ranges around planned output, minimizing unnecessary energy storage system activity during minor fluctuations. The core contribution is a generalized mutual entropy–proximal policy optimization control strategy, which quantifies non-Gaussian tracking errors using generalized mutual entropy while leveraging proximal policy optimization for adaptive learning and improved robustness. Real-world data validation demonstrated significant improvements: 31.6% reduction in average tracking error, 12.6% increase in output compliance within acceptable ranges, 33.4% reduction in maximum tracking error, and approximately 35% fewer ESS charge/discharge cycles. These results confirmed the method's

effectiveness in addressing renewable generation uncertainty while improving tracking performance and extending energy storage system service life.

Keywords: generalized correntropy; reinforcement learning; tracking control, uncertainty and non-Gaussianity; wind-photovoltaic-storage hybrid system

Abbreviations	Full Forms
ESS	Energy storage systems
PV	Photovoltaic
FMPC	Fuzzy Model Predictive Control
GC	Generalized Correntropy
PPO	Proximal Policy Optimization
MPC	Model Predictive Control
MSE	Mean Squared Error
KDE	Kernel Density Estimation
SSE	Sum of Squared Errors
MAE	Mean Absolute Error
PDF	Probability Density Function

1. Introduction

Wind and solar energy represent the two major pillars of renewable energy development, offering significant growth potential for the future energy landscape. However, the inherent intermittency, variability, and unpredictability of these power generation sources result in substantial curtailment of wind and solar resources, presenting critical challenges to the secure, stable operation and economic efficiency of electrical power systems [1,2]. Energy storage systems (ESS) have emerged as a pivotal power regulation technology that effectively addresses the fluctuation issues associated with wind and photovoltaic (PV) generation. These systems offer distinct advantages, including environmental sustainability, high energy density, substantial storage capacity, extended operational lifespan, and operational flexibility [3,4]. Through strategic charging and discharging operations, energy storage systems can absorb excess renewable energy during peak generation periods and release stored energy during periods of low generation, thereby enabling the integrated wind-photovoltaic-storage system to maintain consistent output that aligns with predetermined dispatch schedules. This capability significantly enhances the stability and reliability of the broader electrical power system [5,6].

To optimize the alignment between actual output power and planned output power in wind-photovoltaic-storage hybrid systems, Li et al. [7] developed a model designed to enhance the cosine similarity between planned power curves and the combined power curves of wind, solar, and storage components. Their approach employs a particle swarm optimization algorithm to enable the hybrid system to effectively track planned power output. However, this methodology does not adequately account for the remaining capacity of the energy storage system, potentially resulting in excessive charging and discharging cycles that reduce system lifespan. To address these limitations, Niu et al. [8] proposed an energy storage control strategy for hybrid wind-solar-storage power generation systems. Their approach utilizes fuzzy simulation and dynamic particle swarm

optimization to minimize the error between actual and planned output while maintaining energy storage levels within optimal operational ranges. This methodology optimizes the charging and discharging strategy of energy storage stations to achieve improved tracking of planned output curves. Nevertheless, this method relies solely on instantaneous power data and lacks consideration of future wind and solar power generation forecasts. Building upon these limitations, Qi et al. [9] developed a power scheduling control strategy incorporating fuzzy model predictive control (FMPC) for real-time system optimization. Their approach applies variational mode decomposition technology to analyze the total capacity of the energy storage system, enabling rational power allocation. This methodology effectively reduces deviations between actual and planned power generation while improving the power tracking accuracy of energy storage systems. However, FMPC systems depend on predetermined models and exhibit slow decision update rates, limiting their effectiveness in real-time control applications. In scenarios characterized by extreme fluctuations in wind and solar power outputs, FMPC fails to provide the necessary flexibility for rapid adjustments, consequently affecting tracking accuracy. In contrast, reinforcement learning offers model-independent decision-making capabilities that operate directly based on current system conditions and provide rapid decision outputs, enabling real-time tracking of planned power output. Leveraging these advantages, Zhang et al. [10] implemented a deep deterministic policy gradient algorithm to coordinate power output across wind, photovoltaic, and energy storage systems, ensuring accurate tracking of grid dispatch instructions by the combined system. Through deep reinforcement learning, their approach dynamically adapts to stochastic variations and fluctuations in wind and photovoltaic power generation, thereby achieving real-time, efficient dispatch decisions.

Wind farms and PV power stations within the same region demonstrate observable patterns and correlations [11]. While methods have successfully tracked planned output, they have not adequately addressed the correlation and uncertainty inherent in wind and PV power generation. By comprehensively incorporating these factors, the flexibility and robustness of wind-PV-storage hybrid systems can be significantly enhanced, enabling accurate tracking of planned output across generation scenarios. The Copula function has been extensively utilized to model the dependence between wind and PV power sources [12,13]. Meng et al. [14] developed a wind-PV complementarity coefficient using the Copula function to calculate Spearman and Kendall correlation coefficients, combining these with fluctuation coefficients to assess complementarity across indicators. To address the variability of wind and PV generation scenarios, Liang et al. [15] employed the Copula function to generate output scenarios for both energy sources. Similarly, Xu et al. [16] integrated the Copula method with Gaussian kernel functions to establish a dependence model for wind and PV power systems. These studies provide a robust theoretical foundation for analyzing wind-PV correlation and uncertainty, as well as for optimizing wind-PV-storage energy dispatch. Building on this foundation, Ru et al. [17] developed a probabilistic model for joint wind and PV power using the Copula function, identifying typical output scenarios and implementing an adaptive multi-objective fireworks algorithm with differential selection strategies to enhance environmental-economic dispatch models. Furthermore, Gao et al. [18] generated wind-PV coupled output scenarios based on Copula theory to characterize output fluctuations, subsequently applying an improved particle swarm optimization algorithm to minimize operating costs.

However, the actual output of wind and PV power often exhibits significant non-Gaussian characteristics. Most tracking control strategies rely on traditional error metrics, such as mean squared error (MSE), to quantify the deviation between actual generation and planned output. These

conventional approaches struggle to effectively characterize and manage the non-Gaussian nature inherent in the tracking errors. In contrast, control laws formulated based on information-theoretic criteria, such as Central Error Entropy [19] and Generalized Correntropy (GC) [20], have shown superior performance in handling non-Gaussian disturbances. By incorporating entropy-based measures into the objective function, these methods offer enhanced robustness and improved control accuracy in addressing the complex tracking challenges posed by the stochastic and heavy-tailed behavior of wind and solar power outputs.

Research on wind-PV-storage tracking control systems has not adequately addressed the impact of frequent charge-discharge cycles on the lifespan of energy storage systems. In wind-PV-storage installations, excessive cycling not only reduces battery service life but also increases operational and maintenance costs [21]. To address these challenges, we propose an energy storage control strategy that accounts for wind and PV power uncertainty while achieving planned output tracking. The proposed approach consists of three major components:

(1) **Uncertainty Quantification of Renewable Sources:** Recognizing the correlation and uncertainty inherent in co-located wind and PV generation, a joint probability distribution is constructed using kernel density estimation and Copula functions. This distribution generates numerous correlated scenarios, which are subsequently reduced through K-means clustering to identify representative joint output scenarios for wind and PV systems.
(2) **Interval Control Strategy:** To minimize frequent energy storage cycling within acceptable fluctuation ranges, a deviation band is established around the planned output based on day-ahead power forecasts. This interval control framework prevents unnecessary battery cycling while maintaining system performance.
(3) **Advanced Control Implementation:** A control strategy utilizing Generalized Correntropy-Proximal Policy Optimization (GC-PPO) serves as the core execution layer, providing robust performance under varying operational conditions.

The overall design of GC-PPO will be detailed in the following sections: In Section 2, we describe the wind–PV–storage hybrid system and define the formulated problem. In Section 3, we present the complete GC-PPO scheme, including the construction of the joint distribution model of wind and PV power output, the reduction of model complexity using K-means clustering to identify typical operational conditions, and the development of an optimized control strategy based on proximal policy optimization. In Section 4, we validate the efficacy of the proposed approach using experiments with actual data and include conventional optimal design schemes for fair comparison. Finally, in Section 5, we provide concluding remarks and summarize the key contributions of this research.

2. Problem formulation

2.1. Wind-photovoltaic-storage hybrid system model

The wind-PV-storage hybrid system integrates three major components: A wind power generation subsystem, a PV power generation subsystem, and an energy storage subsystem. The integrated configuration optimizes renewable energy generation and storage capabilities through coordinated operation of these complementary technologies.

The established wind-solar-storage hybrid system architecture is structured as follows:

$$\begin{aligned} &C_{ESS}(t) = C_{ESS}(t-1) + \Delta C_{ESS}(t) \\ &\Delta C_{ESS}(t) = \begin{cases} P_{ESS}(t)\eta_c \Delta t, P_{ESS}(t) \geq 0 \\ P_{ESS}(t)\Delta t / \eta_d, P_{ESS}(t) \leq 0 \end{cases} \\ &P_g(t) = P_{w,pv}(t) + P_{ESS}(t) \end{aligned} \tag{1}$$

where $C_{ESS}(t)$ is the energy storage system residual capacity at time t, $\Delta C_{ESS}(t)$ represent the change in capacity at time t, $P_{ESS}(t)$ is the energy storage system's power output at time t, η_c and η_d are the energy storage system's power output coefficient, respectively, Δt is the sampling time, $P_{w,pv}(t)$ is the actual wind and PV power generation at time t, which has non-Gaussian uncertainty, and $P_g(t)$ is the wind-photovoltaic-storage hybrid system's output power.

2.2. Objective function

To achieve the dual core objectives of extending the lifespan of the energy storage system and ensuring accurate tracking of the planned output, the overall objective function is constructed as the weighted sum of two subobjectives functions: (1) The deviation between the energy storage system's remaining capacity and its ideal capacity, and (2) the deviation between the output power of wind-PV-storage hybrid system and the planned output. However, both aspects must be considered when formulating the objective function.

Regarding the first aspect, due to the limited capacity of the energy storage system, it is essential to account for the variation in its remaining capacity while striving to track the planned output as closely as possible. This consideration is reflected in Eq. (2).

$$J_1 = \sum_{i=1}^{N} | C_{ESS}(i) - C_{ideal} | \tag{2}$$

where $C_{ideal} = \tau \cdot C_R$ is the ideal remaining capacity of the energy storage system, τ is the ideal capacity coefficient, and C_R is the rated capacity of the energy storage system.

To further prolong its service life, frequent charging and discharging operations should be minimized. To this end, an interval control strategy is introduced by defining a reasonable tolerance band around the planned output. If the actual wind and PV power generation falls within this allowable range, the energy storage system remains inactive; i.e., no charging or discharging occurs. Accordingly, based on the day-ahead forecasted power, the planned output is defined as shown in Eq. (3).

$$P_{Plan} = \begin{cases} (1+\omega)P_{Pre}, & P_{w,pv} > (1+\omega)P_{Pre} \\ P_{w,pv}, & (1-\omega)P_{Pre} \leq P_{w,pv} \leq (1+\omega)P_{Pre} \\ (1-\omega)P_{Pre}, & P_{w,pv} < (1-\omega)P_{Pre} \end{cases} \tag{3}$$

where ω is the deviation coefficient, P_{Plan} is the planned output, and P_{Pre} is the day-ahead predicted power.

The second consideration pertains to the operational characteristics of wind-PV-storage hybrid systems, where the combined output of wind and PV power exhibits a non-Gaussian distribution.

Conventional error metrics demonstrate limited effectiveness when addressing non-Gaussian disturbances and inadequately satisfy system requirements for planned output tracking accuracy. Generalized cross-entropy [22] demonstrates superior performance in managing non-Gaussian characteristics. Accordingly, we employ generalized cross-entropy as the metric for quantifying tracking error, as shown in the following equation:

$$J_2 = e(P_g, P_{Plan}) = \frac{\alpha}{2\beta\Gamma(\frac{1}{\alpha})} - \frac{1}{N}\sum_{i=1}^{N}\frac{\alpha}{2\beta\Gamma(\frac{1}{\alpha})}\exp\left(-\left|\frac{P_g(i)-P_{Plan}(i)}{\beta}\right|^{\alpha}\right) \tag{4}$$

where N is 96, representing the 96 time intervals in a day, α is the shape parameter, β is the bandwidth parameter, and $\Gamma(\cdot)$ is the gamma function.

Therefore, the objective function consists of two parts, as shown in Eq. (5):

$$\min J = \omega_1 \cdot J_1 + \omega_2 \cdot J_2 \tag{5}$$

where ω_1 and ω_2 are the weight coefficients. This objective function utilizes statistical information, enabling better adaptation to systems with non-Gaussian characteristics while balancing control accuracy and the service life of the energy storage system.

3. Tracking control strategy for Wind-PV-Storage system based on GC-PPO

The inherent variability and non-Gaussian statistical characteristics of wind and PV power generation present significant challenges for maintaining optimal system performance in hybrid renewable energy systems. To address these uncertainties and improve the tracking accuracy of wind-PV-storage hybrid systems in following planned output trajectories, we propose a novel control strategy based on GC-PPO. The proposed methodology leverages generalized cross-entropy techniques to effectively manage the non-Gaussian probability distributions characteristic of wind and PV power generation profiles. By integrating these techniques with the proven robustness and stability advantages of the Proximal Policy Optimization (PPO) algorithm in reinforcement learning-based policy optimization, the control strategy demonstrates enhanced system tracking performance under conditions of non-Gaussian uncertainty. The comprehensive framework for this approach is presented in Figure 1, illustrating the wind-PV-storage hybrid systems and the advanced control architecture designed to optimize system response to stochastic power generation patterns.

The control scheme for tracking the planned output of the wind-PV-storage hybrid system addresses wind and PV power uncertainty through a three-stage methodology, as detailed in the following subsections.

(a) Probabilistic modeling and scenario generation: The joint distribution of wind and PV power output is modeled using kernel density estimation in conjunction with a copula function. Representative scenarios are generated through random sampling and subsequently reduced using K-means clustering to identify typical operational conditions.

(b) Training algorithm: The identified typical scenarios serve as training samples for the GC-PPO algorithm, enabling the development of an optimized control strategy.

(c) Strategy validation: Ultra-short-term wind and PV forecasts are utilized to generate test scenarios, which validate the effectiveness of the trained control strategy under real-world conditions.

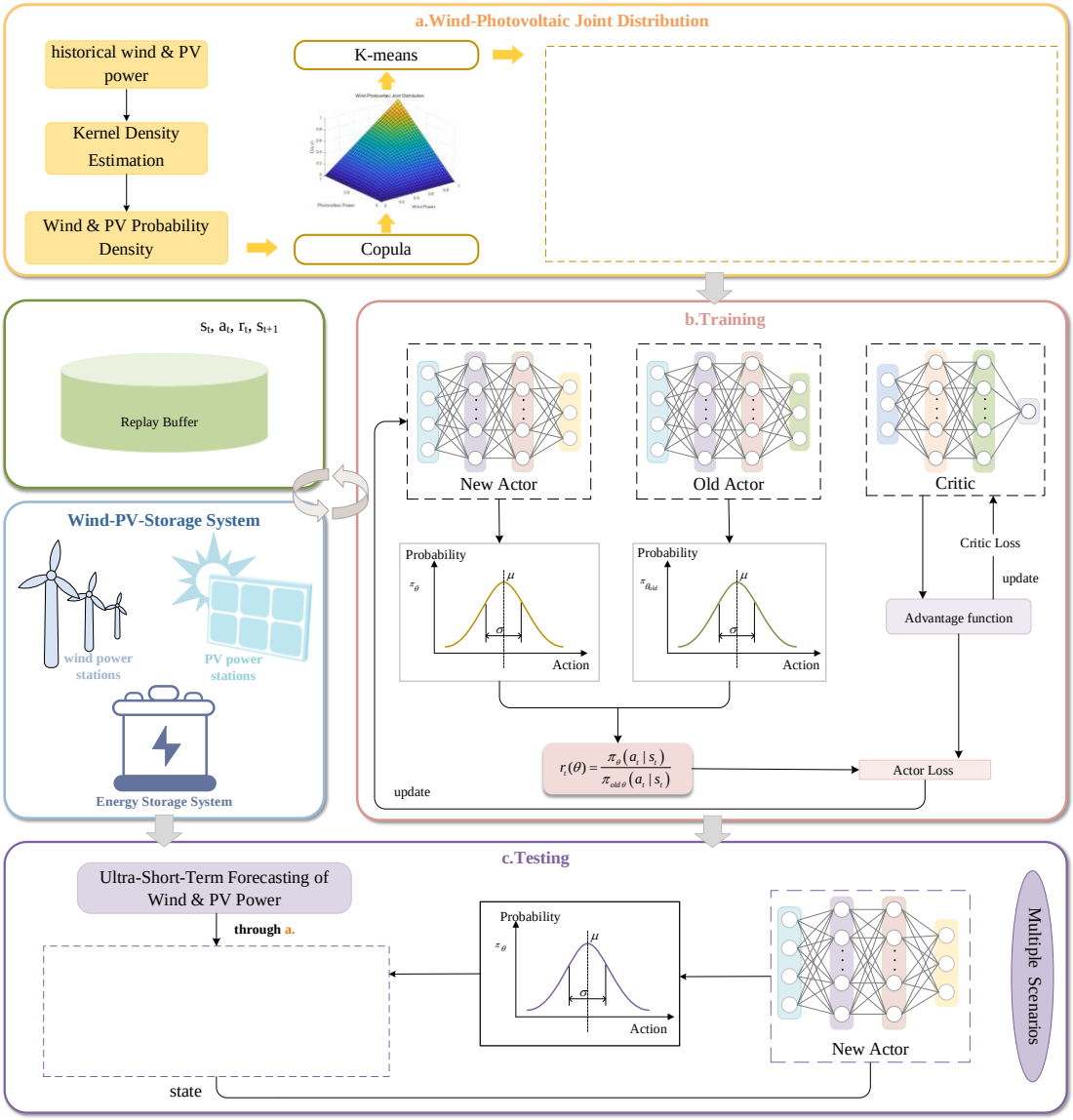

Figure 1. Control scheme for tracking planned output power with Wind and PV uncertainties.

3.1. Modeling the correlation and uncertainty of wind and PV power generation

Wind and PV energy systems are typically distributed across geographical locations within a region. However, their power generation often exhibits strong correlation due to shared meteorological conditions. To characterize the joint distribution of wind and PV power output in a given region, as shown in Figure 2, we employ kernel density estimation (KDE) and copula functions. To reduce computational complexity, the K-means clustering algorithm is then applied to identify representative scenarios from the full dataset, thereby generating typical operational scenarios for analysis. The complete modeling scheme is detailed in this subsection.

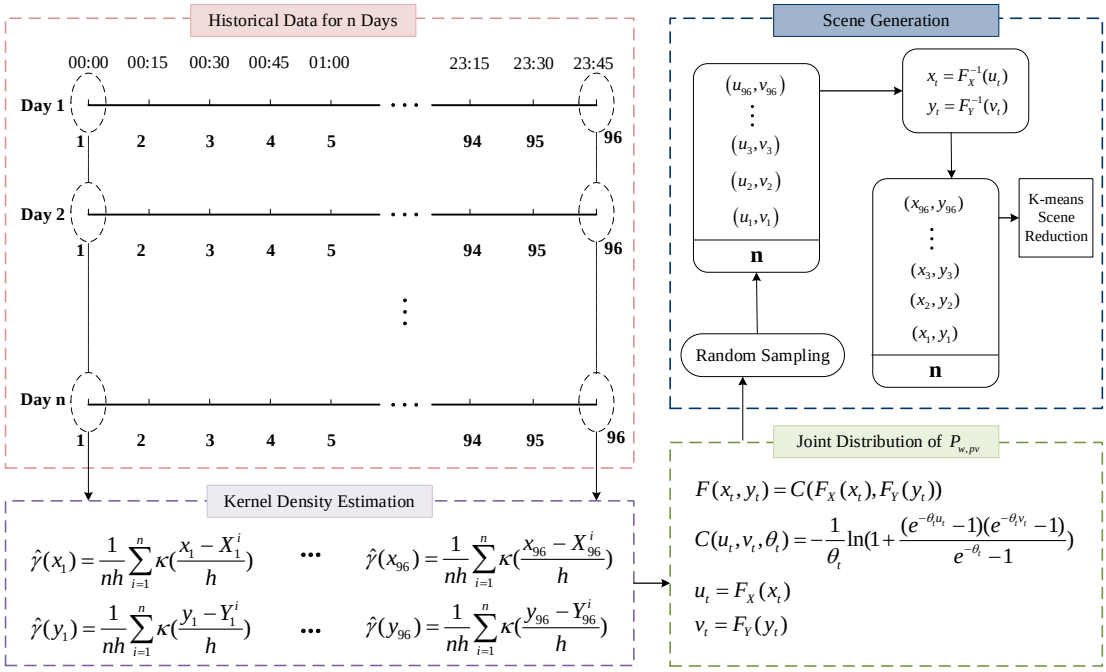

Figure 2. The procedures of wind - PV correlation modeling and scenario generation.

3.1.1. Probability density of wind and PV power based on KDE

The accurate characterization of uncertainty in wind and PV power generation is essential for developing statistically representative stochastic scenarios. Wind and PV power outputs are substantially influenced by meteorological variables, and their probability distributions frequently demonstrate complex non-Gaussian properties. These characteristics present significant challenges when attempting to model power generation patterns using conventional parametric distributions. KDE provides a robust non-parametric approach for capturing the intricate distributional characteristics of renewable energy sources. This method enables more precise representation of the underlying probability structures without the restrictive assumptions inherent in parametric modeling approaches. To address this challenge, we employ KDE [23] to calculate the probability density functions of wind and PV power generation. The wind and solar power sample data are $(x_1,y_1),(x_2,y_2),...,(x_n,y_n)\in(X,Y)$. As illustrated in Figure 2, historical wind and PV power data spanning *m* days are used to construct probability density functions for wind and PV power across 96 discrete time intervals within a 24-hour period. The mathematical formulations for these calculations are presented as follows:

$$\begin{aligned}\hat{\gamma}(x_t)&=\frac{1}{mh}\sum_{i=1}^{m}\kappa(u=\frac{x_t-X_t^i}{h})\\ \hat{\gamma}(y_t)&=\frac{1}{mh}\sum_{i=1}^{m}\kappa(u=\frac{y_t-Y_t^i}{h})\end{aligned}\tag{6}$$

where x_t is the PV power at time t, X_t^i is the PV power at time t on day i, y_t is the wind power at time t, Y_t^i is the wind power at time t on day i, h is the bandwidth, and $\kappa(\cdot)$ is the kernel function, defined as follows:

$$\kappa(u) = \frac{1}{\sqrt{2\pi}} \exp(-\frac{1}{2}u^2) \tag{7}$$

3.1.2. Joint distribution of wind and PV power

After obtaining the probability density functions of PV and wind power, the Copula function is employed to construct their joint distribution. The formulas are presented as follows:

$$F(x_t, y_t) = C(F_X(x_t), F_Y(y_t)) \tag{8}$$

where $F_X(x_t)$ and $F_Y(y_t)$ are the cumulative probability distribution functions of PV power and wind power, respectively, representing the probability that the variable is less than or equal to a certain value. There are many types of Copula functions, such as Frank-Copula, Clayton-Copula, and Gumbel-Copula [24]. To select an appropriate Copula function, correlation coefficients, like the Kendall rank correlation coefficient, Spearman rank correlation coefficient, and squared Euclidean distance, are often used to measure the degree of correlation between variables. They are also used to assess the fit of the Copula functions and select the optimal Copula function that can reflect the correlation between PV and wind power.

(1) Kendall rank correlation coefficient

$$\rho_K = \frac{2(a-b)}{N(N-1)} \tag{9}$$

where a is the number of PV and wind power sample pairs with consistency， b is the number of PV and wind power sample pairs without consistency, and *N* is the total number of sampling points.

(2) Spearman rank correlation coefficient

$$\rho_S = \frac{\sum_{i=1}^{N}(c_i - \bar{c})(d_i - \bar{d})}{\sqrt{\sum_{i=1}^{N}(c_i - \bar{c})^2}\sqrt{\sum_{i=1}^{N}(d_i - \bar{d})^2}} \tag{10}$$

By sorting the PV power samples $X = \{x_1, x_2, \cdots x_N\}$ and the wind power sample $Y = \{y_1, y_2, \cdots y_N\}$ by size, the rank c_i of the *i*-th sample x_i is its position in the sorted order. Similarly, the rank d_i of y_i is its position in the sorted order. Additionally, $\bar{c} = \frac{1}{N}\sum_{i=1}^{N} c_i$ and $\bar{d} = \frac{1}{N}\sum_{i=1}^{N} d_i$.

(3) Squared Euclidean distance

The squared Euclidean distance serves as a goodness-of-fit evaluation metric that quantifies the deviation between the values of the empirical Copula function derived from sample data and the

corresponding values of the theoretical Copula function. The calculation formula is given as follows:

$$d^2 = \sum_{i=1}^{n} [C_s(u_i, v_i) - C_e(u_i, v_i)]^2 \tag{11}$$

where $u_k = F_X(x_k)$, $v_k = F_Y(y_k)$, and $C_s(u,v)$ are the candidate theoretical Copula functions, and $C_e(u,v)$ is the empirical Copula function.

3.1.3. Scenario reduction

Following the establishment of the joint distribution of wind and photovoltaic power, multiple scenarios of wind and PV power samples can be randomly generated. However, the substantial volume of generated power data presents computational challenges that require systematic reduction and scenario selection. To address this issue and identify representative scenarios of joint wind and PV power generation, we employ the *K*-means clustering method [25], a well-established clustering technique.

The K-means algorithm partitions datasets into distinct groups by maximizing intra-cluster similarity while minimizing inter-cluster similarity. This approach serves dual purposes: Organizing and categorizing data while enabling effective data compression. However, the algorithm's performance is critically dependent on the selection of the cluster number (*K*). Inappropriate selection of *K* can result in poor data structure representation, manifesting as either underfitting (insufficient clusters) or overfitting (excessive clusters). Consequently, determining the optimal number of clusters represents a fundamental requirement in developing effective clustering-based analysis and control strategies. To identify the optimal cluster number, we evaluate K-means performance across cluster configurations using established cluster validation metrics that balance intra-cluster compactness with inter-cluster separation. Specifically, the elbow method is implemented for *K* value selection. This approach involves calculating the sum of squared errors (SSE) within clusters for various *K* values, representing the cumulative squared distances from all data points to their respective cluster centroids. The optimal cluster number is determined by analyzing SSE trends as *K* varies, enabling the selection of an appropriate clustering configuration.

3.2. GC-PPO control architecture

Following the derivation of representative scenarios, the output power of the hybrid wind-PV-storage system is optimized to track the planned output through the solution of Eq. (5). However, conventional optimization methods exhibit limited generalization capabilities and are inadequate for addressing the inherent uncertainties associated with wind and PV power generation. Reinforcement learning offers the capability to make adaptive optimization decisions within uncertain environments. Therefore, we employ reinforcement learning to achieve the power tracking objective. Figure 3 presents a schematic representation of the complete reinforcement learning framework. The RL components are formally defined as follows:

(1) The state space encompasses the actual combined power output of wind and PV generation, the planned output trajectory, and the energy storage system's remaining capacity:

$$S(t) = \left\{ P_g(t), P_{Plan}(t), C_{ESS}(t) \right\} \tag{12}$$

(2) The action space consists of the charging and discharging power commands for the energy storage system:

$$A(t) = \{P_{ESS}(t)\} \tag{13}$$

(3) Given the non-Gaussian characteristics inherent in wind and PV power generation, traditional mean error metrics prove inadequate for handling such statistical properties. To address this limitation, generalized cross-entropy is incorporated into the objective function in place of conventional mean error measures. This modification enables more accurate tracking performance under non-Gaussian disturbances by providing a more robust error quantification framework. Consequently, Eq. (5) is reformulated as follows:

$$R = -J = -\omega_1 \mid C_{ESS} - C_{ideal} \mid -\omega_2 \left[\frac{\alpha}{2\beta\Gamma(\frac{1}{\alpha})} - \frac{1}{N}\sum_{i=1}^{N} \frac{\alpha}{2\beta\Gamma(\frac{1}{\alpha})} \exp\left(-\left| \frac{P_g(t) - P_{Plan}(t)}{\beta} \right|^{\alpha} \right) \right] \tag{14}$$

Then, the tracking control problem of wind-PV-storage hybrid systems can be transferred into an optimization problem with the following constraint conditions:

(1) Energy storage system capacity constraints:

$$\begin{aligned} & C_{ESS.\min} \le C_{ESS}(t) \le C_{ESS.\max} \\ & C_{ESS.\min} = C_R \cdot SOC_{\min} \\ & C_{ESS.\max} = C_R \cdot SOC_{\max} \end{aligned} \tag{15}$$

where $SOC_{\min}$ and $SOC_{\max}$ are the lower and upper bounds of the SOC of the energy storage system, and $C_{ESS.\min}$ and $C_{ESS.\max}$ are the lower and upper bounds of the energy storage system's capacity, respectively.

(2) Charging power constraint of the energy storage system:

$$0 \le P_{ESS}(t) \le \min\left[P_R, \frac{C_{ESS.\max} - (1-\rho)C_{ESS}(t)}{\eta_c \cdot \Delta t} \right] \tag{16}$$

(3) Discharging power constraint of the energy storage system:

$$-\min\left[P_R, \frac{((1-\rho)C_{ESS}(t) - C_{ESS.\min}) \cdot \eta_d}{\Delta t} \right] \le P_{ESS}(t) \le 0 \tag{17}$$

where P_R is the rated power of the energy storage system.

(4) Wind and PV power constraints

$$0 \le P_w(t) \le P_{w.\max}$$
$$0 \le P_{pv}(t) \le P_{pv.\max} \tag{18}$$

where $P_{w.\max}$ is the maximum output of the wind power, and $P_{pv.\max}$ is the maximum output of the PV power.

To leverage stable and efficient policy optimization, we employ the PPO algorithm [26]. PPO's primary advantage lies in its ability to restrict the step size of each update through a clipped surrogate objective function, ensuring that policy changes remain within reasonable bounds during each iteration. This approach provides enhanced stability compared to alternative policy optimization methods. To address the non-Gaussian distributions inherent in tracking the planned output of hybrid wind-PV-storage systems, we propose GC-PPO, which combines generalized cross-entropy with the PPO algorithm within the control framework. The designed reward function incorporates generalized cross-entropy to effectively handle the non-Gaussian characteristics of wind and solar power generation. The PPO algorithm enables adaptive iterative optimization of control strategies aimed at tracking the planned output of hybrid wind-solar-storage systems under uncertainty conditions. The comprehensive implementation procedures for the GC-PPO algorithm are presented in Algorithm 1.

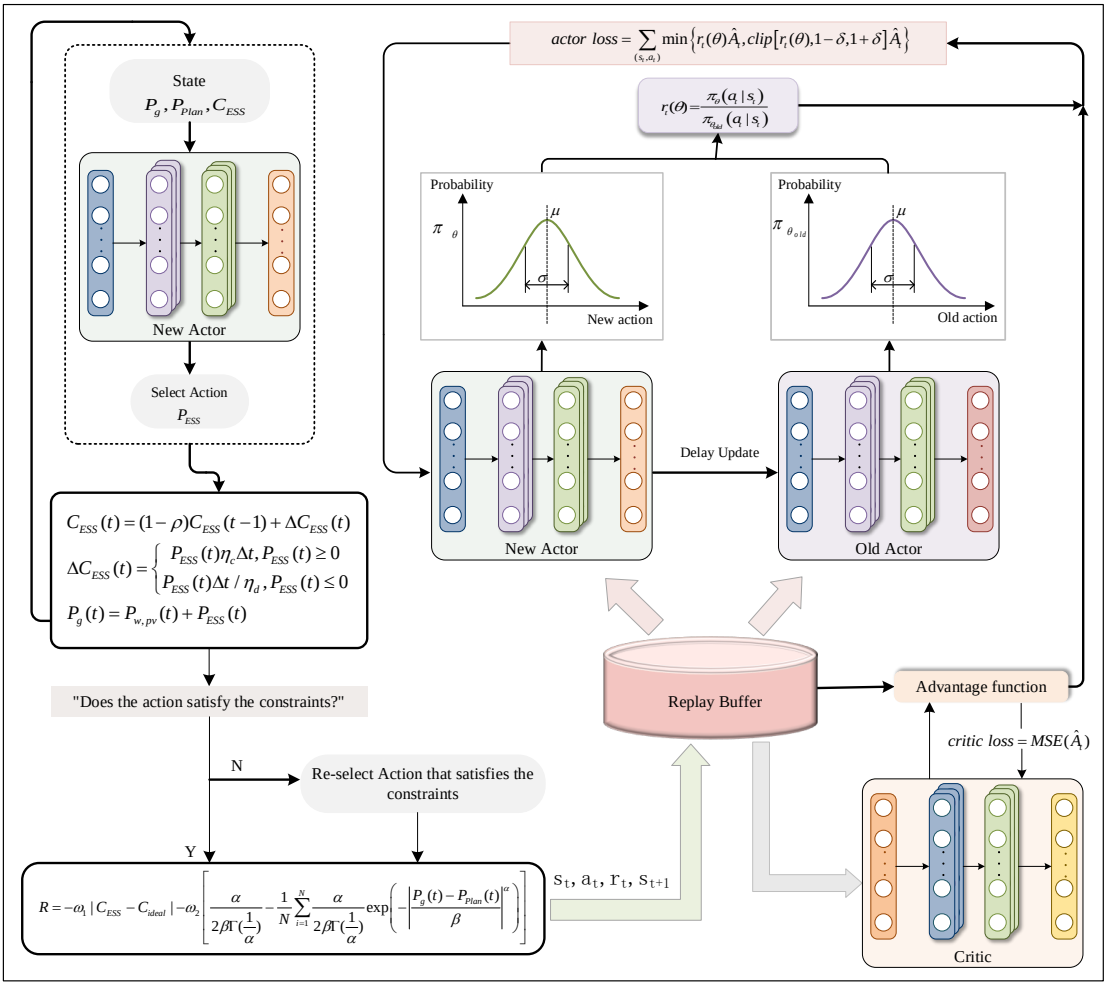

Figure 3. Framework of the GC-PPO algorithm.

Algorithm 1: GC-PPO algorithm

Training:

Initialization: Initialize neural network parameters, the replay buffer *B*, the number of iterations *N*
  for *i* = 1 to *N* do
  Initialize the state s_1
    for *t* = 1 to *T* do
      Select action a_t according to the strategy π_θ
      If action a_t satisfies the constraint, then
        Calculate the reward r_t and obtain the next state s_{t+1}.
        Store the experience tuple (s_t, a_t, r_t, s_{t+1}) into the replay buffer *B*
      else
        Re-select action a_{t_safe}, which satisfies the constraints
        Calculate the reward r_t and obtain the next state s_{t+1}
        Store the experience tuple (s_t, a_{t_safe}, r_t, s_{t+1}) into the replay buffer *B*
      Compute the advantage function $\hat{A}_t$
    end for
    for epoch = 1 to *K* do
      Select mini-batches from the replay buffer *B*
      Update the network parameters θ by the gradient descent method
  end for
  Clear the replay buffer *B*
  end for
  Save the policy parameter θ

Testing:

  Initialize state s_t
  for *t* =1 to *T* do
    Choose the action a_t according to the optimized policy π_θ
    Execute action a_t and update the state to s_{t+1}
end for

The training process enforces strict adherence to operational constraints, requiring the selection of alternative actions whenever constraint violations occur. This constraint enforcement mechanism ensures that all data within the experience pool maintains compliance with established parameters. The framework incorporates interval control methodology through the implementation of permissible fluctuation ranges for planned output, derived from day-ahead power forecasting data. This interval-based approach minimizes the frequency of energy storage system charge-discharge cycles, thereby preserving output tracking accuracy while extending the operational lifetime of energy storage components.

3.3. Evaluation metrics

The performance evaluation framework centers on two major areas: The accuracy of planned output tracking and the operational status of the energy storage system. To comprehensively assess system performance, four key evaluation metrics have been established, with their respective

calculation formulas detailed below.

(1) Probability of allowed range

$$\text{Hit Rate} = \frac{\sum_{t=1}^{N} 1\{(1-\delta)P_{Pre} \le P_g(t) \le (1+\delta)P_{Pre}\}}{T} \tag{19}$$

This metric quantifies the probability that the actual output of the wind-PV-storage hybrid system remains within the predetermined tolerance band of the planned output. A higher metric value indicates superior tracking stability and more reliable adherence to planned generation targets.

(2) Energy storage system output coefficient

$$C_{sc} = \sqrt{\frac{1}{T-1}\sum_{t=1}^{T-1}\left[\frac{C_{ESS}(t)}{C_R} - \tau\right]^2} \tag{20}$$

where T is the total number of charge and discharge cycles of the energy storage system. A smaller value of C_{sc} corresponds to reduced SOC fluctuations within the energy storage system, indicating enhanced stability near the optimal operating point with well-balanced charging and discharging performance. This operational stability enables the system to effectively respond to variability in wind and PV power generation, thereby enhancing the system's flexibility and precision in adhering to planned power output targets.

(3) Average tracking error

$$\overline{e} = \frac{\sum_{t=1}^{N} | P_g(t) - P_{Plan}(t) |}{N} \tag{21}$$

This metric is used to measure the average error between the output of the wind-PV-storage hybrid system and the planned output.

(4) Maximum tracking error

$$e_{\max} = \max | P_g(t) - P_{Plan}(t) | \tag{22}$$

This metric quantifies the average deviation between the actual output of the wind-PV-storage hybrid system and the planned output.

4. Experiment studies

To validate the effectiveness of the proposed GC-PPO tracking control strategy for hybrid wind, PV, and energy storage systems, we present a comprehensive comparative analysis. The evaluation framework employs three distinct control strategies: GC-PPO, MAE-PPO, and Model Predictive Control (MPC), implemented through real-world data training and multi-scenario testing protocols. The experimental methodology focuses on two critical performance metrics: The precision of planned power tracking and the operational characteristics of the energy storage system. This dual-focus approach ensures a thorough assessment of control accuracy and system reliability under varying operational conditions.

4.1. Experimental data and system parameters

The experimental data is derived from the actual operational records of a wind-solar power station in Belgium. The real power and day-ahead forecast data from April to June 2023 are used to train the reinforcement learning agent. To enhance practical relevance, short-term forecast data and day-ahead forecast data from April to June 2024 are used as test data. Specifically, the short-term forecast is used to generate wind-PV power generation scenarios, while the day-ahead forecast is used to develop the generation schedule.

The hybrid renewable energy system consists of a 60 MW wind power facility, a 140 MW PV power station, and an 80 MW energy storage system. The installed capacity of the wind and solar power systems is provided by the power station associated with the adopted dataset. The capacity of the energy storage system is configured based on the actual output data of the wind and photovoltaic power sources, with the core objective of ensuring that the system can effectively accommodate renewable power generation while smoothing power fluctuations. Economic efficiency is also a key consideration in the configuration process, as a larger storage capacity is not inherently advantageous; excessive capacity leads to increased system costs and resource inefficiency. The complete operational parameters for this integrated wind-photovoltaic-storage system are detailed in Table 1.

Table 1. Parameters of the wind-photovoltaic-storage hybrid system.

Parameter	Symbol	Value
rated capacity of the ESS	C_R	80 MW
charging efficiency of the ESS	η_c	1
discharging efficiency of the ESS	η_d	1
sampling time for wind and PV power	Δt	15 min
ideal SOC	τ	0.5
deviation coefficient	ω	0.1
upper limit of the SOC	$SOC_{\max}$	0.8
lower limit of the SOC	$SOC_{\min}$	0.2
rated power of the ESS	P_R	30 MW

4.2. Joint wind and PV power scenario generation

Based on ultra-short-term forecast data spanning April 1, 2024 to June 30, 2024, potential wind and PV power generation scenarios for July 1 are derived using the joint distribution calculation and scenario reduction methodology for wind and solar power output outlined in Section 3.1. The copula function selection process began with a comparative analysis. Table 2 presents the rank correlation coefficients and squared Euclidean distances for five copula function types. The analysis demonstrates that the Frank-Copula exhibits the rank correlation coefficient most closely aligned with the sample data while maintaining a relatively minimal squared Euclidean distance. These characteristics indicate the Frank-Copula's superior capability in capturing the correlation intensity between wind and solar power generation. Consequently, the Frank-Copula is selected for calculating

the wind and PV power's joint distribution.

Table 2. Comparison results of different Copula functions.

	ρ_K	ρ_S	d^2
Frank-Copula	**0.11606**	**0.15861**	0.038781
Clayton-Copula	0.12267	0.18295	0.045529
t-Copula	0.13116	0.18402	0.037614
Gumbel-Copula	0.11659	0.17326	0.039859
Normal-Copula	0.038036	0.057029	0.06755
Sample	0.1186	0.16167	0

The joint distribution function of wind and solar power based on the Frank-Copula is as follows:

$$C(u_t, v_t, \theta_t) = -\frac{1}{\theta_t}\ln(1+\frac{(e^{-\theta_t u_t}-1)(e^{-\theta_t v_t}-1)}{e^{-\theta_t}-1}) \tag{23}$$

where $u_t = F_X(x_t)$, $v_t = F_Y(y_t)$, and θ are the parameters of the Frank-Copula function.

After obtaining the joint distribution of wind and PV power, numerous generation scenarios are randomly sampled from this distribution. The *K*-means clustering method is subsequently applied to reduce the scenario count to a manageable size. Determining the optimal number of clusters (*K* value) requires analysis of the underlying data distribution characteristics. The elbow method is employed to select the appropriate *K* value by calculating the SSE within clusters for various *K* values. The SSE represents the sum of squared distances from all data points to their respective cluster centroids. Through examination of SSE trends as *K* varies, an optimal cluster number can be identified. The SSE decreases progressively as *K* increases; however, the rate of decrease diminishes correspondingly. Beyond a certain *K* value, the SSE reduction rate slows considerably, creating an inflection point known as the "elbow" position. The *K* value corresponding to this elbow represents the optimal cluster number. Selecting excessively large *K* values, while continuing to reduce SSE, may result in model overcomplexity and increased computational burden. The elbow method effectively mitigates overfitting risks. As demonstrated in Table 3, the SSE decline rate becomes approximately constant when *K* reaches 5. Consequently, to minimize computational requirements while maintaining model effectiveness, *K* = 5 is selected as the optimal cluster number.

Table 3. Rate of decline of SSE for different K values.

K value	2	3	4	**5**	6	7	8	9	10
decline rate	36.27	28.74	20.21	**20.35**	15.86	15.50	16.12	16.29	15.71

Figure 4 presents the reduced wind and PV power generation scenarios obtained through *K*-means clustering analysis. These scenarios preserve the stochastic characteristics of renewable energy output while maintaining statistical representativeness through systematic cluster selection. This approach enables the quantification of probable generation profiles for wind and PV power systems.

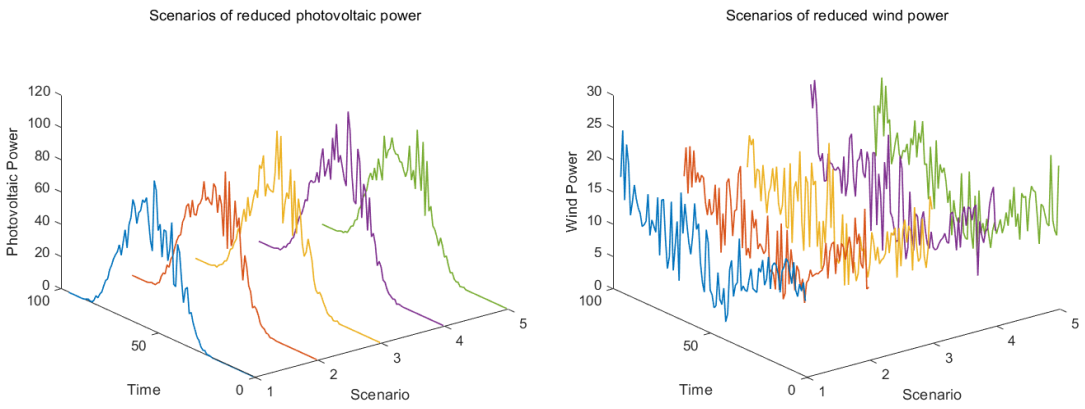

Figure 4. Wind and PV power generation scenarios.

To elucidate the physical drivers underlying these output profiles, Table 4 provides meteorological interpretations corresponding to each clustered scenario.

Table 4. Weather characteristics of typical scenarios.

Typical Scenario	Meteorological Type	Weather Type
Scenario 1	moderate wind speed, moderate-to-low irradiance	cloudy weather
Scenario 2	low wind speed, low irradiance	overcast weather
Scenario 3	moderate wind speed, high irradiance	sunny with breeze weather
Scenario 4	rapidly changing wind speed and irradiance	severe convective weather
Scenario 5	high wind speed, moderate irradiance	windy weather

4.3. Training parameters and objectives

We employ three control strategies as comparative benchmarks: GC-PPO, MAE-PPO, and MPC. MAE-PPO is the same as GC-PPO, except that the GC term in GC-PPO is replaced with mean absolute error (MAE) term in MAE-PPO. MPC is same as MAE-PPO but it is optimized by the conventional gradient method. The training objectives are separately established for all strategies, wherein each strategy must dynamically optimize the charging and discharging power of energy storage systems through continuous learning of key operational parameters. These parameters include the current actual output of wind and solar power generation, the planned output targets, and the SOC of the energy storage system. The primary optimization goals are twofold: First, to minimize tracking error between actual and planned output, and second, to maximize the operational lifespan of the energy storage system. The training parameters utilized for the GC-PPO implementation are detailed in Table 5.

Table 5. GC-PPO algorithm training parameters.

Parameter	Value
Batch size	128
Episode	2000
Discount factor	0.9
Learning Rate of Actor Network	0.00001
Learning Rate of Critic Network	0.0001
Clipping parameter	0.2
Shape parameter	1.5
weight coefficients	0.1, 0.9

4.4. Simulation results and analysis

4.4.1. Verification of GC-PPO's handling of non-gaussian characteristics

Figure 5 illustrates the three-dimensional evolution of the tracking error PDF during the GC-PPO training process. As the number of training steps increases, the PDF curve corresponding to a tracking error of zero becomes increasingly concentrated and sharp, indicating that the model's tracking accuracy continuously improves as errors gradually converge toward zero. The evolution from an initially broad distribution to a final sharp peak visually demonstrates that the proposed GC-PPO algorithm effectively captures the non-Gaussian characteristics of wind and PV power output through generalized correntropy measurement, thereby reducing wind-solar power tracking errors and enhancing overall tracking accuracy.

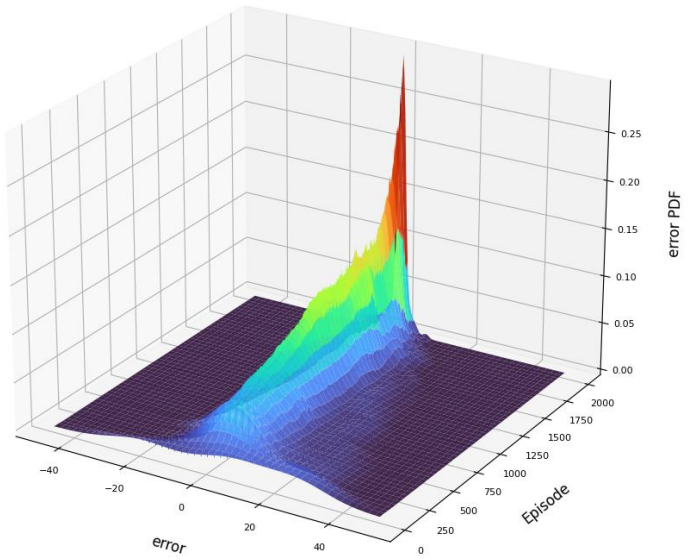

Figure 5. Evolution of error PDF in GC-PPO.

To demonstrate the superior performance of the GC-PPO strategy, a representative scenario is analyzed. Figure 6 illustrates the tracking performance of planned output power, while Figure 7 presents the variation in remaining capacity of the energy storage system. As shown in Figure 6, the GC-PPO strategy maintains output power within the planned range more consistently than the

MAE-PPO and MPC methods. The energy SOC variation shown in Figure 7 indicates that while the MPC method achieves SOC values closer to the ideal target of 0.5, the GC-PPO strategy maintains SOC fluctuations within acceptable limits.

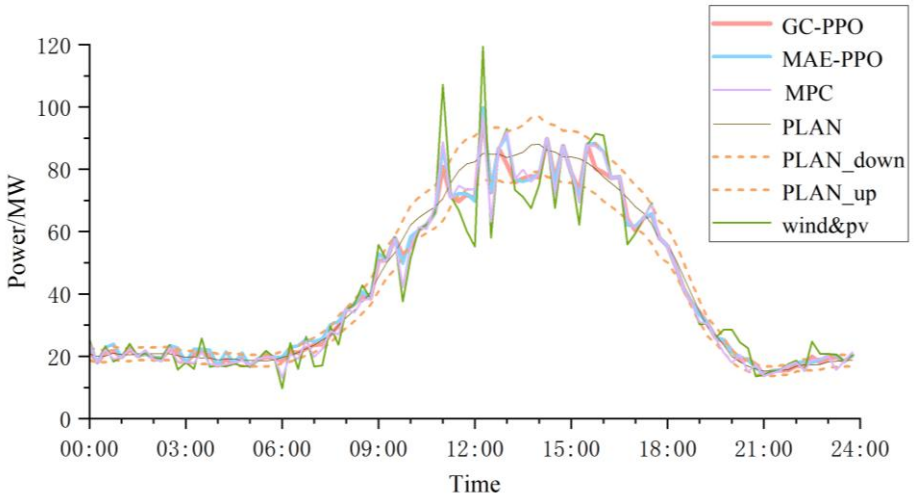

Figure 6. Output power of the wind-PV-storage system under different control strategies.

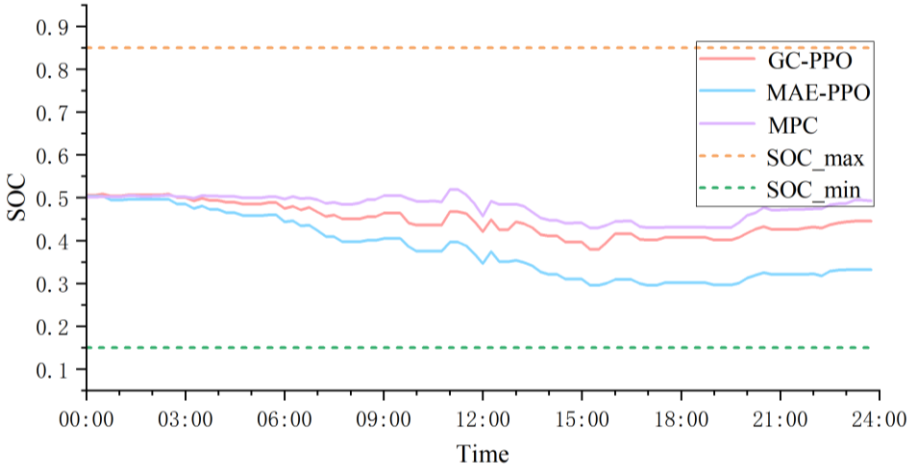

Figure 7. SOC variation of the ESS with different control strategies.

To provide a more quantitative assessment of tracking errors across the three control strategies, Figure 8 presents the probability density function (PDF) of errors at final convergence for each approach. The GC-PPO method exhibits the narrowest PDF distribution with the highest peak concentration, indicating superior tracking control performance. In contrast, the MAE-PPO and MPC methods demonstrate reduced effectiveness in managing wind and PV power generation characterized by non-Gaussian distributions, resulting in comparatively suboptimal tracking performance.

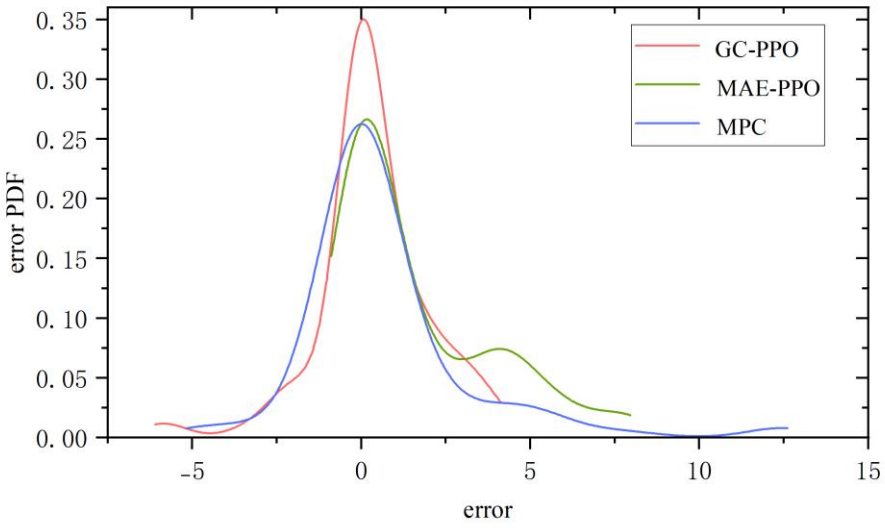

Figure 8. PDF of the tracking error under different control strategies.

While MPC demonstrates a marginal advantage in SOC stability, this benefit is insufficient to offset its diminished tracking accuracy during periods of non-Gaussian fluctuations. In contrast, the GC-PPO algorithm achieves substantial improvements in tracking accuracy with only minimal SOC trade-offs, while maintaining compliance with the energy storage system's safe operating constraints. Although MPC exhibits SOC values closest to the theoretical ideal, GC-PPO demonstrates superior overall tracking accuracy despite a slight reduction in SOC performance. Consequently, when considering tracking precision and energy storage system longevity, the GC-PPO strategy represents a more advantageous solution.

To provide a quantitative comparison of tracking performance among three control strategies under wind and PV power output uncertainty, evaluation metrics are calculated across five distinct scenarios, as presented in Tables 6-10.

Table 6. Performance evaluation indices (Scenario 1).

	Hit Rate (%)	C_{sc}	$\overline{e}$ (MW)	$e_{\max}$ (MW)	$t(s)$
GC-PPO	**88.54**	**0.1587**	**0.4438**	**5.8414**	0.110
MAE-PPO	77.08	0.2191	0.5856	8.0526	**0.045**
MPC	63.12	0.1822	0.5005	12.6095	2.162

Table 7. Performance evaluation indices (Scenario 2).

	Hit Rate (%)	C_{sc}	$\overline{e}$ (MW)	$e_{\max}$ (MW)	$t(s)$
GC-PPO	**81.25**	0.0610	**0.5972**	**7.8931**	0.052
MAE-PPO	73.95	0.1652	0.9986	13.9158	**0.048**
MPC	66.25	**0.0485**	1.0319	10.1588	2.199

Table 8. Performance evaluation indices (Scenario 3).

	Hit Rate (%)	C_{sc}	$\overline{e}$ (MW)	$e_{\max}$ (MW)	$t(s)$
GC-PPO	**81.25**	0.0678	**0.3945**	**6.1354**	0.124
MAE-PPO	72.91	0.1116	0.6263	9.8991	**0.056**
MPC	67.29	**0.0554**	0.6732	10.0668	2.149

The analysis reveals that GC-PPO achieves the highest tracking accuracy across all five scenarios, indicating that the wind-solar-storage hybrid system output remains within the planned output range with a superior probability compared to the MAE-PPO and MPC strategies. Furthermore, the average tracking error $\overline{e}$ and maximum tracking error $e_{\max}$ under GC-PPO are substantially lower than those observed with MAE-PPO and MPC. These results demonstrate that GC-PPO effectively addresses non-Gaussian uncertainty in wind-solar output by leveraging the combined advantages of generalized correntropy for handling non-Gaussian characteristics and the adaptive optimization capabilities of the PPO algorithm. This integration enables real-time response to system changes, continuous optimization of the decision-making process, and minimization of tracking errors and system fluctuations. While MAE-PPO employs PPO to address uncertainty, its inability to handle non-Gaussian characteristics results in suboptimal tracking performance. Although GC-PPO exhibits slightly longer runtime compared to MAE-PPO, this difference remains within acceptable limits for practical applications, particularly given its superior overall performance. MPC demonstrates the poorest tracking performance under wind-solar generation uncertainty due to its fixed optimization model and limited real-time feedback capability, which restricts the flexibility required to effectively manage system uncertainty.

Table 9. Performance evaluation indices (Scenario 4).

	Hit Rate (%)	C_{sc}	$\overline{e}$ (MW)	$e_{\max}$ (MW)	$t(s)$
GC-PPO	**85.42**	0.1053	**0.4758**	**4.1423**	**0.045**
MAE-PPO	73.96	**0.0715**	0.8886	7.9659	0.050
MPC	64.17	0.0963	0.7086	9.9154	1.994

Table 10. Performance evaluation indices (Scenario 5).

	Hit Rate (%)	C_{sc}	$\overline{e}$ (MW)	$e_{\max}$ (MW)	$t(s)$
GC-PPO	**83.33**	0.1035	**0.4850**	**5.5923**	**0.049**
MAE-PPO	75	0.1787	0.5118	6.0965	**0.049**
MPC	67.29	**0.0768**	0.6405	9.4725	2.339

Regarding energy storage system operation, the energy storage output coefficients C_{sc} under GC-PPO are lower than those of MAE-PPO across all five scenarios, indicating that GC-PPO employs a more balanced charging and discharging strategy. This provides enhanced flexibility in available capacity utilization and contributes to an extended energy storage system lifespan. In Scenario 4, the energy storage output coefficient C_{sc} for GC-PPO marginally exceeds that of

MAE-PPO; however, this difference remains within acceptable limits given GC-PPO's significantly superior tracking accuracy in this scenario. Although MPC demonstrates the lowest energy storage output coefficient C_{sc} in most scenarios, it exhibits significant limitations in tracking accuracy and computational runtime. Consequently, MPC lacks the robustness necessary to adapt to uncertain operating conditions and, due to inadequate real-time performance, fails to satisfy the fundamental requirements for real-time dynamic control in wind-solar-storage integrated systems. Overall, the comparative analysis demonstrates that GC-PPO delivers optimal performance for wind-solar-storage hybrid system control under uncertainty, offering superior tracking accuracy, balanced energy storage utilization, and acceptable computational efficiency for real-time applications.

Based on the ultra-short-term forecast data from April 1 to June 30, 2024, five possible joint wind-PV power generation scenarios for July 1 are generated using the method described in Section 3.1. These five scenarios are subsequently employed to evaluate the tracking performance of the power generation plan for July 1, validating that the GC-PPO algorithm exhibits favorable tracking performance. To further verify the generalization capability of the algorithm, tracking performance is also assessed using the corresponding power generation plans for July 2 through July 4. Table 11 presents the performance evaluation results for these three days. The results demonstrate that the GC-PPO algorithm maintains stable and consistent tracking performance across power generation plans of different dates, confirming its adaptability and generalization capability in responding to fluctuations in practical application scenarios.

Table 11. Tracking performance indices of the GC-PPO algorithm under different power generation plans.

	Hit Rate (%)	C_{sc}	$\overline{e}$ (MW)	$e_{\max}$ (MW)	$t(s)$
GC-PPO(Plan1)	88.54	0.1587	0.4438	5.8414	0.110
GC-PPO(Plan2)	83.33	0.1298	0.5955	4.8686	0.050
GC-PPO(Plan3)	85.41	0.1486	0.5292	5.4755	0.044

4.4.2. Verification of the effectiveness of interval control

Figure 9 illustrates the charging and discharging power profiles of the energy storage system under three control strategies with interval control, compared to the GC-PPO control strategy without interval control. Table 12 presents the charging and discharging cycle counts for the energy storage system under the GC-PPO strategy with interval control and the GC-PPO strategy without interval control across five operational scenarios. The results demonstrate that the implementation of interval control mechanisms substantially reduces the frequency of charging and discharging cycles compared to strategies without interval control. This reduction mitigates degradation caused by frequent cycling operations, enabling the energy storage system to maintain periods of operational rest between power adjustments, thereby extending its operational lifespan. The interval control methodology ensures that deviations between the hybrid wind-solar-energy storage system output and the planned output remain within acceptable tolerance limits. By achieving satisfactory tracking performance while minimizing energy storage system wear, this approach effectively prolongs the service life of the energy storage infrastructure.

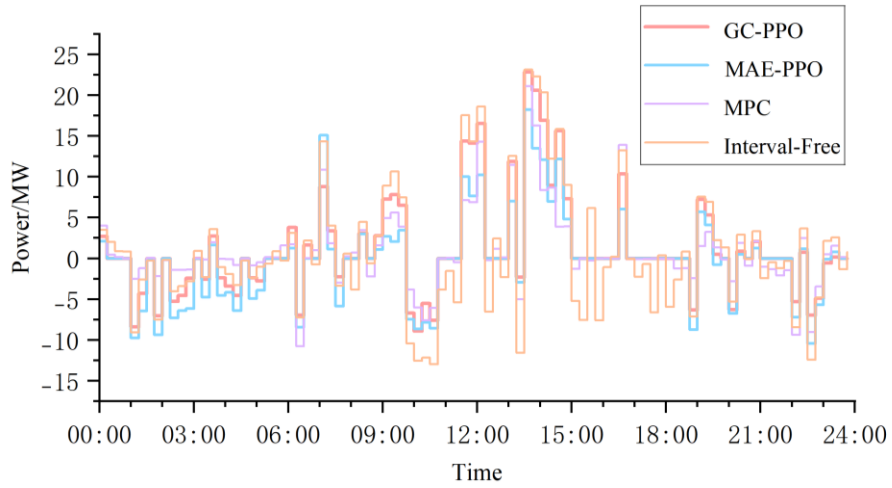

Figure 9. Charging and discharging power of the energy storage system.

Table 12. Number of charging and discharging cycles of the energy storage system.

Control Strategy	Scenario 1	Scenario 2	Scenario 3	Scenario 4	Scenario 5
GC-PPO (Interval-Free)	96	96	96	96	96
GC-PPO (Interval)	60	70	65	54	71

Experimental results show that compared with other control methods, the GC-PPO control strategy demonstrates superior tracking performance in the five typical scenarios: The average tracking error is reduced by 31.6%, the probability of staying within the allowable range of planned output is increased by 12.3%, and the maximum tracking error is reduced by 41.4%. This verifies its robust tracking ability under the non-Gaussian uncertainty of wind and PV power. Moreover, the introduction of interval control reduces the number of energy storage charging and discharging cycles by an average of about 35%, effectively reducing energy storage wear while ensuring tracking accuracy, achieving dual optimization of tracking performance and energy storage life. Furthermore, the implementation of interval control methodology results in an approximate 35% reduction in energy storage charging and discharging cycles. This optimization effectively minimizes energy storage degradation while preserving tracking accuracy, thereby achieving simultaneous improvements in tracking performance and energy storage longevity.

5. Conclusions

In this paper, we address critical challenges in hybrid wind-PV-storage power generation systems, focusing on wind-PV correlation, output uncertainty, non-Gaussian characteristics, and the frequent charging-discharging cycles of energy storage systems during planned output tracking operations. We employ Copula functions combined with KDE to calculate the joint probability distribution of wind and solar power outputs, enabling quantification of correlation patterns and uncertainty characteristics inherent in renewable energy generation. K-means scenario reduction technology is implemented to manage computational complexity while preserving essential statistical properties of the renewable energy sources. A novel GC-PPO control strategy is proposed to

effectively address the non-Gaussian and stochastic nature of wind and PV power generation, resulting in enhanced planned output tracking performance. Additionally, an interval control mechanism is integrated to substantially reduce the frequency of energy storage charging-discharging operations, thereby extending system lifespan and improving operational efficiency. The research presents three major innovations:

- **Enhanced Non-Gaussian Uncertainty Handling:** Generalized correntropy is incorporated into the objective function to leverage its robust characterization of non-Gaussian distributions. This advancement enables more accurate quantification of tracking errors between wind-PV-storage system output and planned targets, improving control accuracy in non-Gaussian operational scenarios.
- **Battery Life-Optimized Interval Control:** A novel interval control methodology establishes appropriate fluctuation ranges for planned output. When renewable generation falls within predetermined thresholds, energy storage system actions are actively suppressed. Beyond these limits, the system executes charging-discharging operations to rapidly correct deviations. This approach maintains tracking precision while preventing excessive cycling, thereby extending battery service life.
- **Integrated GC-PPO Control Framework:** The proposed framework addresses correlation and uncertainty in renewable power generation through two key mechanisms. First, generalized correntropy manages non-Gaussian characteristics of wind and PV output. Second, the adaptive capabilities of the PPO algorithm address generation uncertainty through stable policy optimization and high sample efficiency, enabling rapid adaptation to uncertain operational scenarios. The integration of generalized correntropy ensures robust control performance under non-Gaussian and uncertain conditions.

We effectively address key challenges in hybrid wind-PV-storage power generation systems, including output correlation, non-Gaussian uncertainty, and frequent energy storage cycling, through an innovative framework integrating Copula-based probabilistic modeling with GC-PPO intelligent control. The proposed control mechanism significantly reduces energy storage degradation while maintaining tracking accuracy, achieving coordinated optimization of system tracking performance and economic lifespan. This work provides a novel technical approach for ensuring secure and stable operation of high-proportion renewable energy power systems.

Although this study has achieved promising results in planned output tracking control, limitations remain. First, while we aim to extend energy storage lifespan by reducing charge-discharge cycles, we do not incorporate precise battery aging models or comprehensive lifecycle economic cost analysis, which limits the quantitative assessment of lifespan extension. Second, we focus on single-timescale tracking control and do not address the coordinated operation of wind-PV-storage systems across intraday timeframes or under multi-objective scenarios.

In future studies, researchers could develop an energy storage optimization model that integrates electrochemical aging mechanisms with economic analysis, and expand to a hierarchical control framework featuring multi-timescale and multi-objective coordination. This would enable balanced optimization of lifecycle costs and comprehensive operational benefits while enhancing tracking performance.

Author contributions

Yujing Shi: Writing – original draft, Software, Methodology; Mifeng Ren: Writing – review & editing, Vali dation, Funding acquisition; Lan Cheng: Conceptualization, Investigation; Jianhua Zhang: Methodology, Conceptualization; Junghui Chen: Writing – original draft, Writing – review & editing, Methodology, Formal analysis, Investigation.

Use of Generative-AI tools declaration

The authors declare they have not used Artificial Intelligence (AI) tools in the creation of this article.

Acknowledgments

The authors would like to gratefully acknowledge the Fundamental Research Program of Shanxi Province (202203021222124).

Conflict of interest

All authors declare no conflicts of interest in this paper.

References

1. Liu B, Lund JR, Liao S, Jin X, Liu L, Cheng C (2020) Optimal power peak shaving using hydropower to complement wind and solar power uncertainty. *Energ Convers Manage* 209: 112628. https://doi.org/10.1016/j.enconman.2020.112628
2. Yu Q, Gao S, Sun G, Qin R (2023) Optimization of wind and solar energy storage system capacity configuration based on the Parzen window estimation method. *J Renew Sustain Energ* 15. https://doi.org/10.1063/5.0172720
3. Rekioua D (2023) Energy storage systems for photovoltaic and wind systems: A review. *Energies* 16: 3893. https://doi.org/10.3390/en16093893
4. Choopani K, Effatnejad R, Hedayati M (2020) Coordination of energy storage and wind power plant considering energy and reserve market for a resilience smart grid. *J Energy Storage* 30: 101542. https://doi.org/10.1016/j.est.2020.101542
5. Deepa R, Shakila Devi GT, Balamurugan KS (2025) Hybrid photovoltaic wind renewable energy sources for microgrid using osprey optimization algorithm and augmented physics informed neural network. *J Renew Sustain Energ* 17. https://doi.org/10.1063/5.0257110
6. Yin S, Chen S, Pan N, Bu Y, Lin C, Yang J (2025) Optimization of multi-energy collaborative economic operation in plateau zero-carbon parks considering the consumption of wind and solar energy. *J Renew Sustain Energ* 17. https://doi.org/10.1063/5.0289642
7. Li H, Wang S, Gao J (2019) Research on Energy Storage Control Strategy of Wind Solar Storage Combined Generation System Based on Tracking Plan. *Electrical & Energy Management Technology*, 71–78. https://doi.org/10.16628/j.cnki.2095-8188.2019.04.013
8. Niu R, Guo J, Li X, Shu J, Ma X, Liu L (2020) Energy storage control strategy of

wind-photovoltaic-storage hybrid system. *Therm. Power Gener* 49: 150–155. https://doi.org/10.19666/j.rlfd.202005142

9. Qi X, Li X, He S (2018) FMPC-VMD Based Control Strategy for Tracking Generation Plans of Multi-type Energy Storage System. *In 2018 China International Conference on Electricity Distribution (CICED)*, 2253–2259. https://doi.org/10.1109/ciced.2018.8592371
10. Zhang S, Ma C, Yang Z, Wang Y, Wu H, Ren Z (2023) Deep Deterministic Policy Gradient Algorithm Based Wind-Photovoltaic-Storage Hybrid System Joint Dispatch. *Electric Power* 56: 68–76.
11. Yin Q, Wang Z, Sun T, Li W, Chong F (2019) Environmental and economic dispatch with photovoltaic and wind power. *In 2019 IEEE Sustainable Power and Energy Conference (iSPEC)*, 1108–1112. https://doi.org/10.1109/ispec48194.2019.8975242
12. Wang Z, Zhu H, Zhang D, Goh H, Dong Y, Wu T (2023) Modelling of wind and photovoltaic power output considering dynamic spatio-temporal correlation. *Applied Energy* 352: 121948. https://doi.org/10.1016/j.apenergy.2023.121948
13. Lin S, Liu C, Shen Y, Li F, Li D, Fu Y (2021) Stochastic planning of integrated energy system via Frank-Copula function and scenario reduction. *IEEE T Smart Grid* 13: 202–212. https://doi.org/10.1109/tsg.2021.3119939
14. Meng J, Dong Z, Zhu S (2025) A copula-based wind-solar complementarity coefficient: Case study of two clean energy bases, China. *Energy* 318: 134904. https://doi.org/10.1016/j.energy.2025.134904
15. Liang Y, Ma H, Liang Z, Wang H, Li J (2024) A method for configuring hybrid electrolyzers based on joint wind and photovoltaic power generation modeling using copula functions. *Sustain Energy Grids* 40: 101539. https://doi.org/10.1016/j.segan.2024.101539
16. Lanjing X, Zhiwei W, Yanfeng L (2017) The spatial and temporal variation features of wind-sun complementarity in China. *Energy Convers Manage* 154: 138–148. https://doi.org/10.1016/j.enconman.2017.10.031
17. Ru Y, Wang Y, Mao W, Zheng D, Fang W (2024) Dynamic Environmental Economic Dispatch Considering the Uncertainty and Correlation of Photovoltaic–Wind Joint Power. *Energies* 17: 6247. https://doi.org/10.3390/en17246247
18. Gao F, Bao D, Zhao M, Wang T, Xu J (2025) Smoothing Characteristic of Wind-Solar Coupled Output Fluctuations by Hybrid Energy Storage under Multi-Scenario Planning. *Transactions of China Electrotechnical Society* 40: 2827–2839. https://doi.org/10.19595/j.cnki.1000-6753.tces.241679
19. Ren M, Cheng T, Chen J, Xu X, Cheng L (2016) Single neuron stochastic predictive PID control algorithm for nonlinear and non-Gaussian systems using the survival information potential criterion. *Entropy* 18: 218. https://doi.org/10.3390/e18060218
20. Zhang J, Zhou S, Ren M, Yue H (2016) Adaptive neural network cascade control system with entropy-based design. *IET Control Theory Appl* 10: 1151–1160. https://doi.org/10.1049/iet-cta.2015.0992
21. SUN L, DANG S, LIU G, WANG S, HU P (2025) A frequency-modulation power optimization method for energy storage power stations considering the transition state of charge-discharge and power constraints. *Energy Storage Science and Technology* 14: 1286–1298. https://doi.org/10.19799/j.cnki.2095-4239.2024.1191
22. Chen L, Qu H, Zhao J (2018) Generalized Correntropy based deep learning in presence of

non-Gaussian noises. *Neurocomputing* 278: 41–50. https://doi.org/10.1016/j.neucom.2017.06.080
23. Heer, J (2021) Fast & accurate gaussian kernel density estimation. *In 2021 IEEE Visualization Conference (VIS)*, 11–15. https://doi.org/10.1109/vis49827.2021.9623323
24. Ismail I, Abd Mutalip F NN, Jacob K (2023) A comprehensive review on the development of copulas in financial field. *J Intell Fuzzy Syst* 45: 604–-6062. https://doi.org/10.3233/jifs-223481
25. Sinaga KP, Yang MS (2020) Unsupervised K-means clustering algorithm. *IEEE access* 8: 80716–80727. https://doi.org/10.1109/access.2020.2988796
26. Elumalai VK (2025) A proximal policy optimization based deep reinforcement learning framework for tracking control of a flexible robotic manipulator. *Results in Engineering* 25: 104178. https://doi.org/10.1016/j.rineng.2025.104178

AIMS Press